



RESEARCH ARTICLE

# Technology-driven chickpea yield estimation using remote sensing and crop modeling

Sellaperumal Pazhanivelan<sup>1\*</sup>, A Ragul<sup>2</sup>, NS Sudarmanian<sup>1</sup>, S Satheesh<sup>3</sup>, Kancheti Mrunalini<sup>4</sup> & KP Ragunath<sup>1</sup>

<sup>1</sup>Centre for Water and Geospatial Studies, Tamil Nadu Agricultural University, Coimbatore 641 003, Tamil Nadu, India

<sup>2</sup>Agro Climate Research Centre, Tamil Nadu Agricultural University, Coimbatore 641 003, Tamil Nadu, India

<sup>3</sup>Department of Remote Sensing and GIS, Tamil Nadu Agricultural University, Coimbatore 641 003, Tamil Nadu, India

<sup>4</sup>Indian Council of Agricultural Research-Indian Institute of Pulses Research, Kanpur 208 024, Uttar Pradesh, India

\*Correspondence email - [pazhanivelans@gmail.com](mailto:pazhanivelans@gmail.com)

Received: 22 December 2024; Accepted: 25 January 2025; Available online: Version 1.0: 26 May 2025; Version 2.0 : 09 June 2025

**Cite this article:** Sellaperumal P, Ragul A, Sudarmanian NS, Satheesh S, Mrunalini K, Ragunath KP. Technology-driven chickpea yield estimation using remote sensing and crop modeling. *Plant Science Today*. 2025; 12(2): 1-14. <https://doi.org/10.14719/pst.6859>

## Abstract

This study estimated chickpea area and yield in Vidisha district, Madhya Pradesh, during Rabi 2022-23 by integrating Sentinel-1A SAR satellite data with the CROPGRO-Chickpea crop simulation model. Sentinel-1A VH-polarized GRD data (20 m spatial resolution) were processed using MAPscape software at 12-day intervals. Temporal backscatter analysis identified distinct growth-stage signatures, enabling accurate crop classification. The total classified chickpea area was 109112 ha. Classification accuracy was 86.8 %, with a Kappa coefficient of 0.74. The DSSAT model simulated chickpea growth and yield, with maximum Leaf Area Index ranging from 1.8 to 4.9 and yields from 1410 to 2449 kg ha<sup>-1</sup>. Remote sensing-based chickpea yield estimates ranged between 1420 and 2330 kg ha<sup>-1</sup>. Validation showed strong agreement between observed and simulated values, with accuracies of 89.1 % for LAI and 91.7 % for yield. This study underscores the effectiveness of integrating remote sensing and crop modelling for precise, scalable agricultural monitoring, supporting sustainable crop management and food security.

**Keywords:** chickpea yield; DSSAT; remote sensing, sentinel-1A; temporal backscatter

## Introduction

Chickpea is a globally significant pulse crop valued for its high nutritional content, with seeds containing 15 - 22 % protein, 50 - 58 % carbohydrate and essential micronutrients (1, 2). It is the third most cultivated pulse crop worldwide, with an annual production of 11.6 million tonnes, of which India contributes 64 % (3, 4). Madhya Pradesh ranks first in chickpea cultivation in India, accounting for 28 % of the total sown area and 34 % of national production (5). Accurate crop area and yield estimation are essential for food security planning, especially for staple crops like chickpeas. Traditional field survey methods, while commonly used, are labour-intensive, expensive and susceptible to errors. Remote sensing (RS) technologies provide an efficient and reliable alternative, enabling large-scale and precise crop monitoring. RS data are extensively used in agriculture for crop growth assessment, stress detection and yield forecasting due to their broad spatial coverage, rapid data acquisition and cost-effectiveness (6, 7).

Combining optical and synthetic aperture radar (SAR) data enhances the accuracy of remote sensing applications in agriculture. Optical data provide critical vegetation indices such as NDVI and LAI but are limited by weather conditions. In contrast, being weather-independent, SAR data allows

continuous monitoring of key crop parameters such as biomass and plant structure (6). Advancements in SAR sensor technology and automated processing have significantly improved crop mapping and monitoring, including for chickpeas. Crop simulation models, such as those in the Decision Support System for Agrotechnology Transfer (DSSAT), further enhance yield estimation by simulating crop growth and yield dynamics using soil, weather and management data. Integrating RS data with crop simulation models has been demonstrated as a robust approach for spatial yield estimation (8, 9). This study integrates SAR remote sensing and the DSSAT-CROPGRO-Chickpea model to map chickpea cultivation and estimate yield in Vidisha district, Madhya Pradesh.

## Materials and Methods

### Study area

The research area comprises Vidisha district in Madhya Pradesh. Vidisha is one of the 52 districts in Madhya Pradesh, covering an area of 737100 ha (Fig. 1). Vidisha is located at 23.5236° N latitude and 77.8140° E longitude in Central India. It is bordered to the northeast by Ashoknagar, to the east by Sagar and Raisen, to the south by Bhopal and the northwest by Guna.

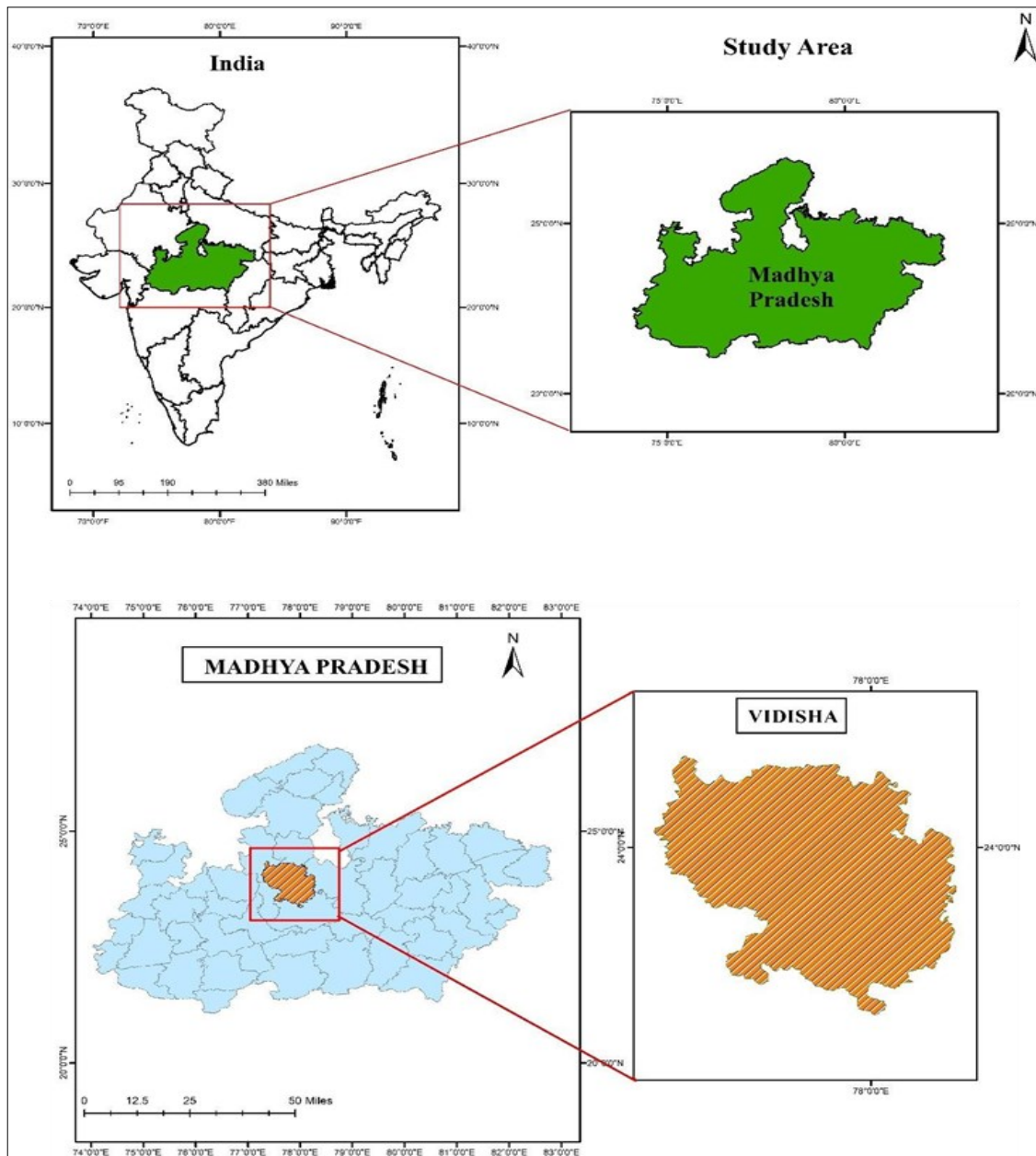


**Fig. 1.** The location map of the Study area – Vidisha.

### Ground truth data

Ground truth data were collected at different stages of chickpea growth during the growing season in the Vidisha district. Ground truth data were used for training and validation to enhance the accuracy of chickpea area mapping. Locations were selected where the surrounding 1 ha land cover was homogeneous and at least 50 m away from roads, populated areas and other infrastructure (10). One hundred and fifty chickpea crop points and 100 other crop points were collected during the ground survey for training and validation. Ground truth points for Vidisha are in Fig. 2. Out of the 150 chickpea points collected, 20 were selected as monitoring sites for training the DSSAT model in the Vidisha district. The monitoring site locations are shown in Fig. 3.

### Chickpea crop area estimation

#### Satellite data

A major advantage of Synthetic Aperture Radar (SAR) is its ability to capture data day and night, irrespective of cloud cover or lighting conditions. The C-SAR instrument aboard

Sentinel-1 facilitates frequent and continuous wide-area monitoring. Sentinel-1s' C-band imaging system operates in 4 distinct modes-Strip Map, Extra Wide Swath, Interferometric Wide (IW) Swath and Wave Mode-each providing different resolutions and coverage areas (Fig. 4). It features rapid data delivery, dual-polarization capability and a short revisit time. Sentinel-1A/1B SAR Ground Range Detected (GRD) datasets with VH polarization in Interferometric Wide (IW) swath mode are acquired at 12-day intervals for crop identification and mapping in the study region. Fig. 5. provides an overview of Sentinel-1A/1B acquisition and coverage over the research area. Table 1 presents the properties of Sentinel 1 satellite data. Fig. 6 displays a crop calendar illustrating chickpeas' main growth stages and planting dates. To obtain complete coverage for the crop growth time in the research area, the Sentinel-1A satellite data were downloaded from <https://scihub.copernicus.eu/dhus/> between October 2022 - March 2023 based on the typical chickpea growing season in the area.

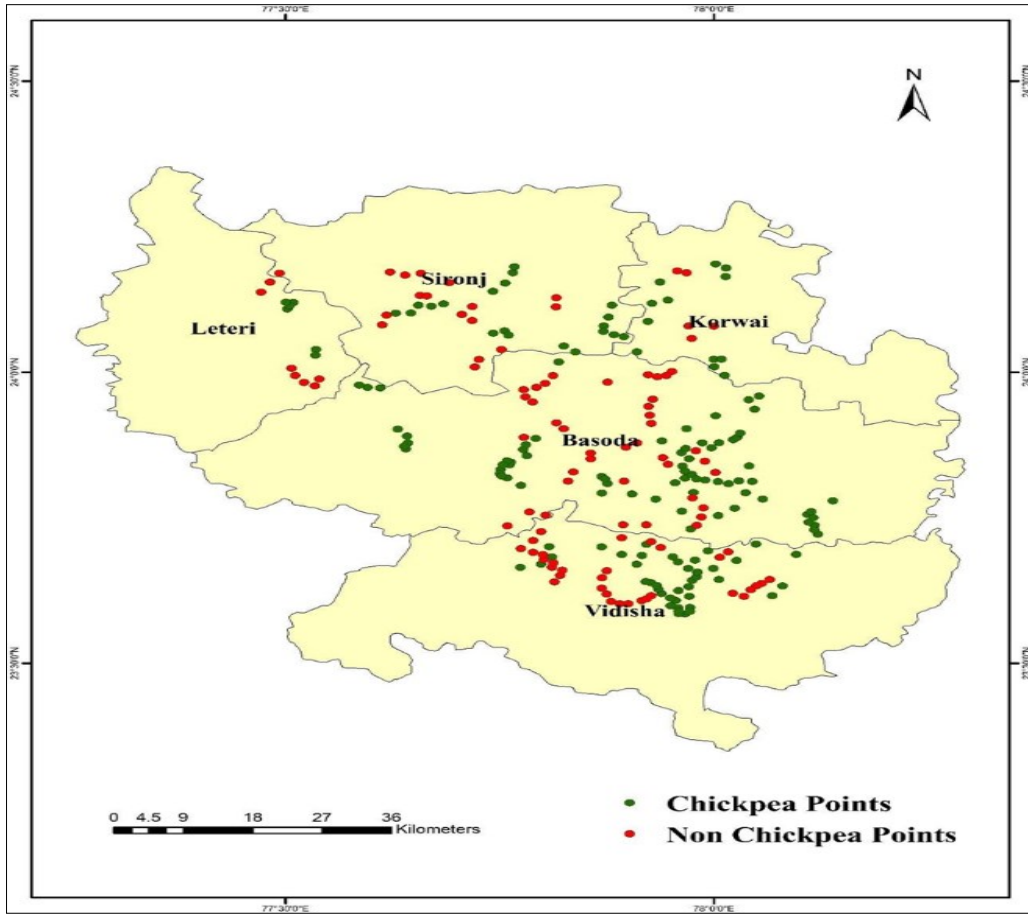


Fig. 2. Ground truth points in the study area.

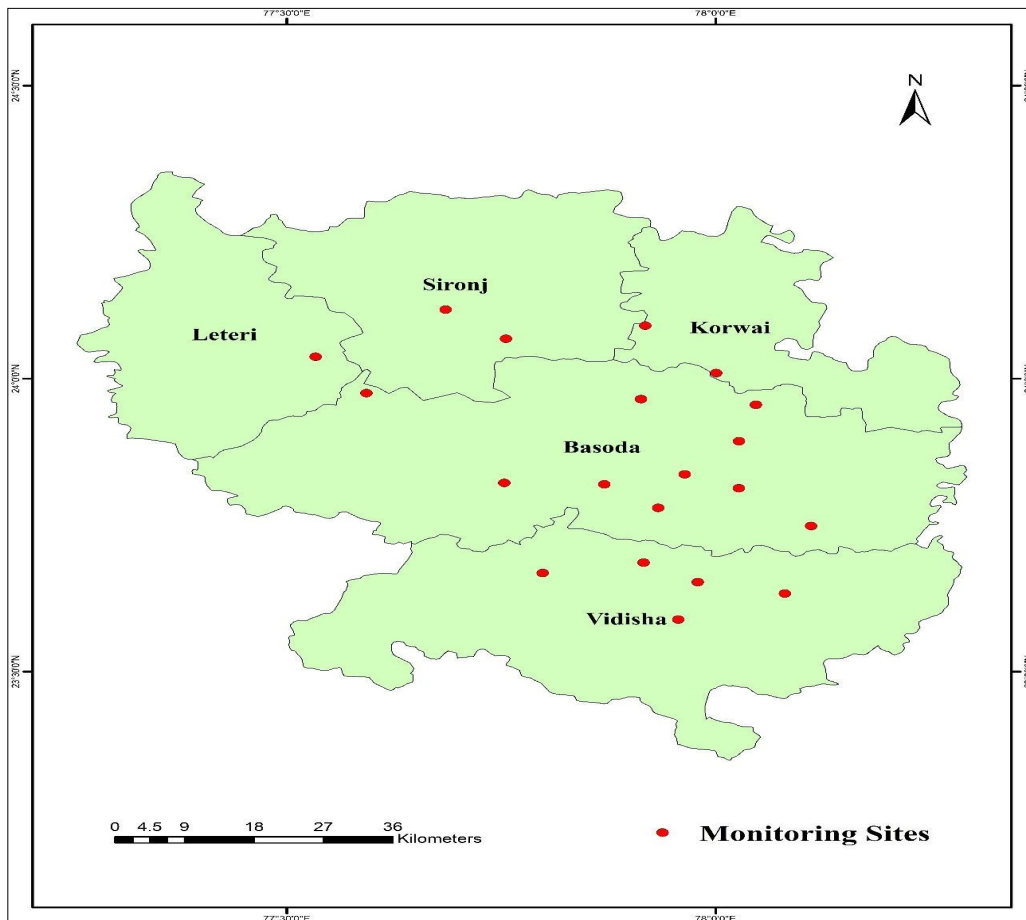


Fig. 3. Location of monitoring sites in the study area.

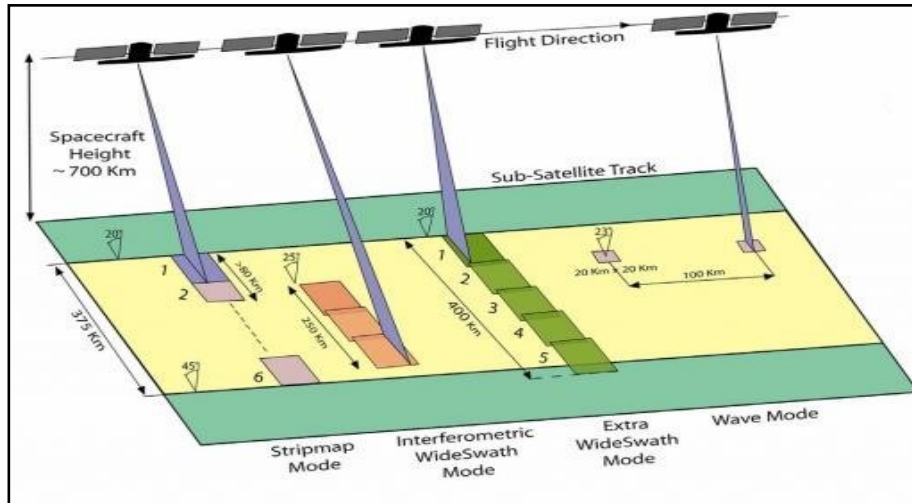


Fig. 4. Sentinel-1A satellite product modes.

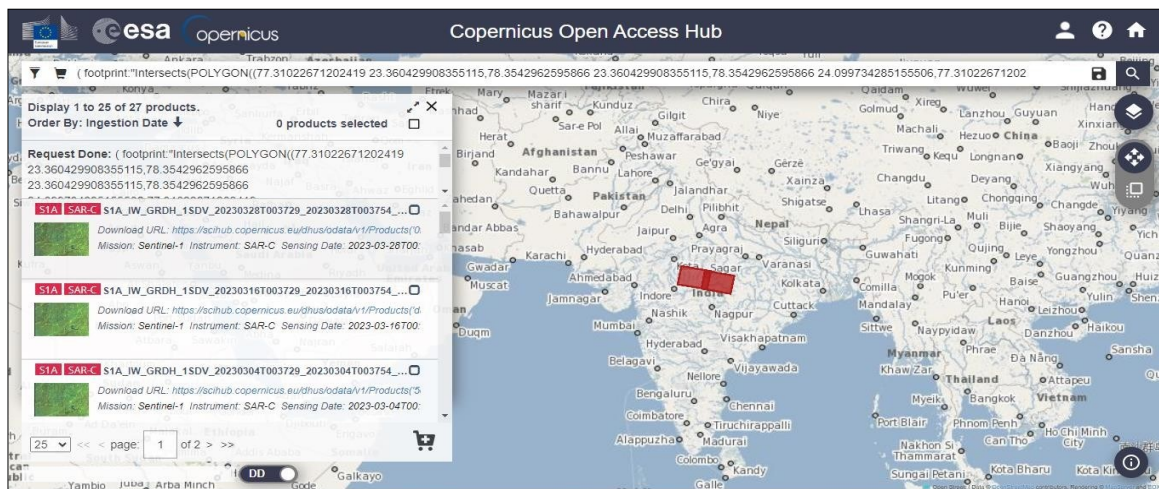


Fig. 5. Overview of Sentinel-1A acquisition and coverage in the study area-Vidisha.

**Basic processing of time series SAR data**

Sentinel-1A/1B SAR Ground Range Detected (GRD) multi-temporal data were processed using an automated chain in MAPscape software to obtain topography geo-coded backscatter values ( $\sigma^0$ ) following the methodology (11). Key pre-processing steps included:

**Strip mosaicking**

Merging SAR datasets of the same orbit and acquisition date into continuous strips to simplify processing.

**Co-registration**

Aligning images with consistent observation geometry in slant range format ensures accurate spatial comparison and analysis.

**Time-series speckle filtering**

Using a multi-temporal filter reduces noise and balances reflectance variations across time (12).

**Terrain geocoding, calibration and normalization**

Geocoding is performed using Digital Elevation Model (DEM) data and calibration is ensured using the radar equation. Range dependency was corrected by applying incidence angle normalization. Incidence angle normalization was applied to correct range dependency.

**Anisotropic non-linear diffusion filtering**

Enhancing target homogeneity while smoothing image regions (13).

Table 1. Characteristics of Sentinel-1A data

Parameters	GRD
Pixel value	Magnitude detected
Coordinate system	Ground range
Polarizations	Single (VH), Cross (VV)
Ground range coverage (km)	251.8
Radiometric resolution (dB)	1.7
Bits per pixel	16
Resolution (range × azimuth) (m)	20.4 × 22.5
Pixel spacing (range × azimuth) (m)	10 × 10
Incident angle	32.9°
Number of looks	5 × 1
Range look bandwidth (MHz)	14.1
Azimuth look bandwidth (Hz)	315
Equivalent number of looks (ENL)	4.4
Absolute location accuracy (m) GRD	7

### Atmospheric attenuation correction

Interpolating and correcting anomalies caused by water vapour and rainfall (14).

### Subsetting

Restricting raster images to the Vidisha district to streamline processing.

### Multi-temporal feature extraction

The feature extraction tool in the MAPscape software retrieved multi-temporal characteristics, including "Minimum, Maximum, Mean, Minimum date, Maximum date and Span ratio" of VH polarization data. These multi-temporal features, which were retrieved using QGIS 2.18.20's point sampling tool, have a specific range of the chickpea crop.

### Maximum likelihood classification (MLC)

The Maximum Likelihood Classification (MLC) method classifies an unknown pixel by statistically analyzing the variance and covariance of spectral response patterns for each category. It assumes a Gaussian distribution for the training dataset, allowing the mean vector and covariance matrix to characterize each class' distribution. Based on these parameters, the statistical likelihood of a pixel belonging to a specific class can be determined.

The image was initially classified using the MLC method applied to multi-temporal stacked SAR images to identify chickpeas. The classification process integrated multi-temporal SAR images to develop spectral signatures for chickpea crops using training pixels collected from various locations. Special emphasis was placed on VH polarization to enhance classification accuracy (Fig. 7). This method successfully distinguished chickpea fields from other land cover types, demonstrating its robustness for agricultural mapping.

### Accuracy assessment

The classification accuracy can be evaluated using the error matrix and Kappa statistics. To determine the classification accuracy, each pixel in a classified picture is compared to the proper class allocation on reference data. The validation method takes 40 % of the total ground reference data and the pixels of agreement and disagreement are integrated into an error matrix. The matrix elements correspond to the number of pixels in the testing dataset and the rows and columns reflect the total number of classes (15).

The confusion matrix was utilized to assess accuracy metrics, including overall accuracy (Eqn. 1), producer accuracy (Eqn. 2) and user accuracy (Eqn. 3) (16). These accuracy measures were estimated to evaluate classification performance. Overall accuracy, representing the percentage of correctly classified instances along the diagonal, was computed as follows:

Overall accuracy =

$$\left( \frac{\text{Total Correctly Classified Pixels}}{\text{Total Number of Pixels}} \right) \times 100 \quad (\text{Eqn. 1})$$

User's accuracy =

$$\left( \frac{\text{Number of Correctly Classified Pixels in a Category}}{\text{Total Number of Pixels Classified into That Category}} \right) \times 100 \quad (\text{Eqn. 2})$$

Producer's accuracy =

$$\left( \frac{\text{Number of Correctly Classified Pixels in a Category}}{\text{Total Number of Reference Pixels in that category}} \right) \times 100 \quad (\text{Eqn. 3})$$

### Integration of Sentinel-1A satellite data and DSSAT model

#### DSSAT Crop simulation model

The development of DSSAT resulted from international partnership work done under IBSNAT, USA (17). Crop, soil and weather databases are combined into standard forms by the microcomputer software product DSSAT for evaluation by crop models and application programmes. The DSSAT was employed in the current study because it allows users to simulate the results of crop management strategies over several years for various crops in any place in the world. In Fig. 8 the methodology of DSSAT yield estimation.

#### CROPGRO-Chickpea module

The crop growth and development were simulated on a daily time step by the CROPGRO-Chickpea module which was included in DSSAT v. 4.8. With the help of infiltration, irrigation, vertical drainage, soil evaporation, unsaturated flow, plant transpiration and root water uptake, this model calculates daily variations in soil water content in a soil layer. Cultivar coefficients were needed as input to the simulation model.

#### Different Input data for the DSSAT model

##### Weather data

Daily weather data, including solar radiation ( $\text{MJ m}^{-2} \text{ day}^{-1}$ ), Wind (m/s), minimum and maximum temperatures ( $^{\circ}\text{C}$ ) and rainfall (mm), were converted into the DSSAT weather file format using the Weather Man tool.

##### Soil data

Soil profile data specific to the study area were extracted from the DSSAT soil database, which provides soil information at a 1:10000 scale. The S Build tool in the CROPGRO model was utilized to generate a simulation soil file.

##### Crop management data

The crop management file, generated using the X Build tool in DSSAT, included information on experimental conditions and field characteristics such as planting geometry, irrigation, fertilizer management, tillage operations and harvest management. This file also specified environmental modifications and simulation control parameters.







Crop	Oct 2022	Nov 2022	Dec 2022	Jan 2023	Feb 2023	Mar 2023
Chickpea						
	Sowing to Branching				Flowering to Pod Formation	
	Branching to Flowering				Pod Formation to Maturity	
				Maturity to Harvest		

Fig. 6. Crop calendar of chickpea.

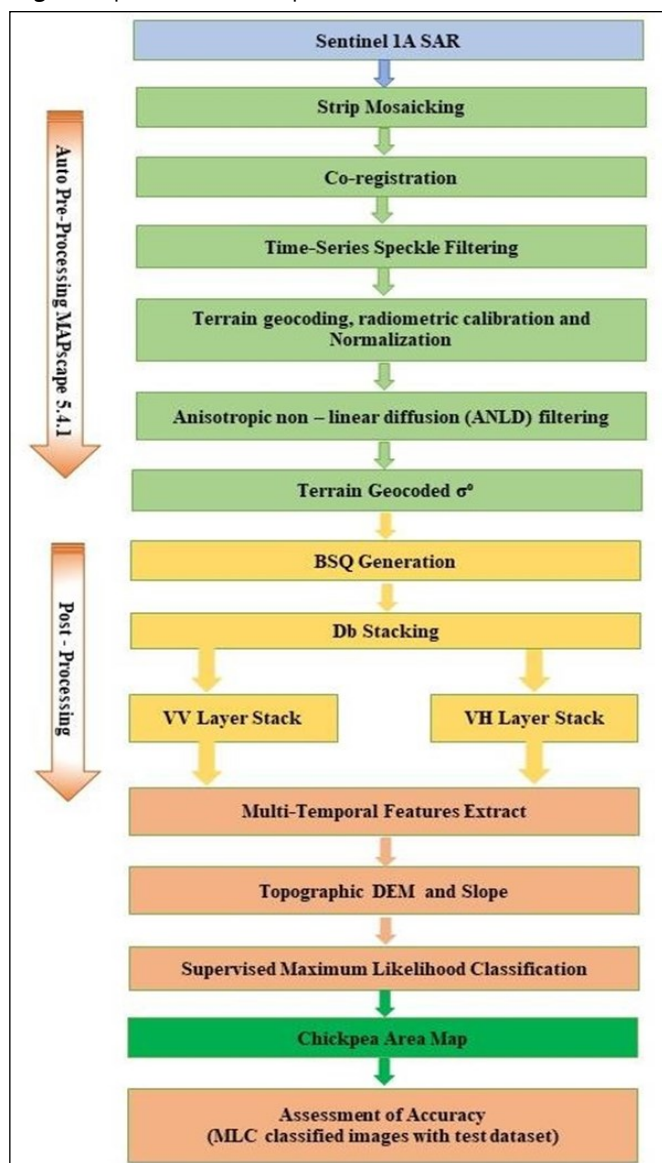


Fig. 7. Flow chart depicting chickpea area mapping methodology.

#### Cultivar file

A Cultivar file describing the genetic coefficient for the cultivars JG 16, JAKI 9218, RVG 202 and JG 218 for Vidisha was used. The genetic characteristics include CSDL (Critical Short-Day Length below which reproductive development progresses with daylength effect (for long day plants), PPSN (Slope of the relative response of development to photoperiod with time (negative for long day plants), EM-FL (Time between plant emergence and flower appearance), etc.

#### Model calibration and validation

Three input files were compiled to execute the DSSAT model with the gathered datasets.

#### Weather file

Generated using the 'Weatherman' program in DSSAT with collected weather data.

#### Soil file

Created using the s' Build' program in DSSAT with soil data.

#### Experimental data file

Developed using the 'X Build' program in DSSAT, incorporating crop management data. The model was calibrated using data obtained during 2021 chickpea crop growing season to compute the genetic coefficient for JG 16, JAKI 9218, RVG 202 and JG 218 with spatial analysis mode in DSSAT. The crop growth model was proved accurate by comparing the predicted output with the actual yield. The observed yield data is the actual yield data that were collected from a farmers' field in the study area. A variety of quality standards were used to assess the simulation results. To quickly assess modeling accuracy, linear regression and the correlation coefficient were used to generate graphs comparing observed and simulated yield values.

#### Generation of leaf area index for chickpea yield estimation

The development of Leaf Area Index (LAI) and crop yields should be simulated using a method that requires the least input data and is based on the physiological and phenological mechanisms that control these qualities in plants. There have been 2 methods created to solve this issue: The LAI is typically calculated using remote sensing techniques or the LAI was directly measured by calculating the length and width of the fully expanded apical leaflet of the third trifoliate leaf at 30-day intervals, starting from 30 days after sowing (DAS) until harvest (18).

$$LAI = \frac{L \times W \times B \times \text{Number of leaves}}{\text{Spacing (cm)}} \quad (\text{Eqn. 4})$$

Where,

L- Length of the leaf (cm)

W-Width of the leaf (cm)

K-Constant factor (0.65)

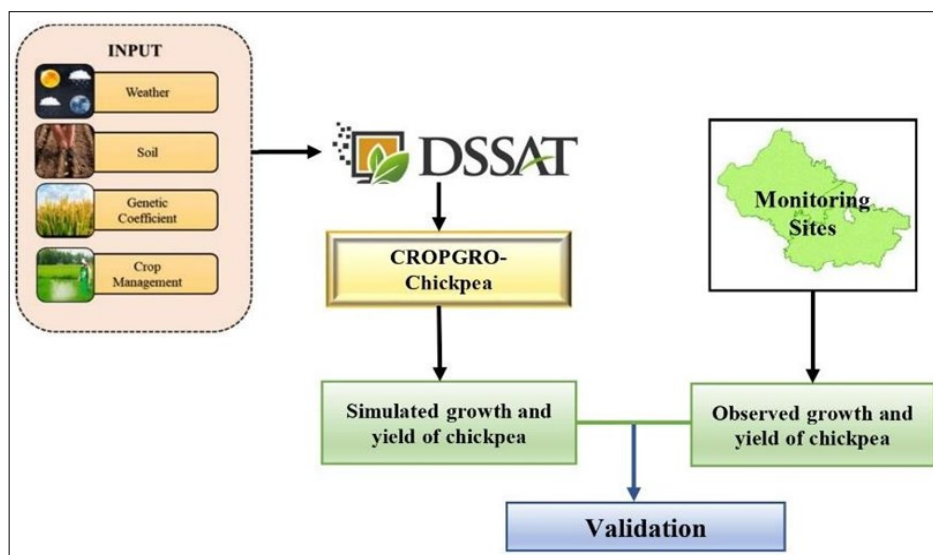


**Fig. 8.** Schematic representation of methodology of DSSAT CROPGRO-Chickpea crop simulation model.

Three LAI measurements were collected from each field and the mean value was determined. Data on yields from each field was logged at the end of the growing season. To provide information to the CROPGRO-Chickpea module for simulation and validation purposes, the entire dataset was finally completed with 20 points across the study region. The 20 Points were continuously monitored using the CROPGRO model point-based spatial LAI and yield was estimated.

#### Retrieving LAI from SAR data

We used the point sampling tool in QGIS 2.18.20 to monitor chickpea fields to extract dB (backscattering) values from SAR data. Using this data, we developed a linear regression model to establish a relationship between dB values and the simulated LAI values for the study region. The QGIS raster calculator tool was used to create selection queries, apply Map Algebra syntax and perform mathematical calculations with operators and functions. These tools generated a spatial LAI map of the study area. LAI values were derived from the DSSAT CROPGRO-Chickpea model and the regression

relationship was used to convert dB values from the crops' blooming phases into corresponding LAI values. This process was performed using the raster calculator to create a geographically distributed LAI dataset.

#### Spatial estimation of chickpea yield through integration of Sentinel-1A data and the CROPGRO model

Fig. 9 illustrates the integration of Sentinel-1A SAR data with the CROPGRO simulation model for estimating chickpea yield. This approach integrated DSSAT-simulated yield with remote sensing data using LAI values extracted from Sentinel-1A dB images. A regression equation was developed to estimate yield by correlating regionally simulated LAI values with DSSAT-simulated yield in the study area. This integration enabled spatial yield mapping by linking biophysical parameters derived from the SAR data with crop model outputs, improving yield prediction accuracy.

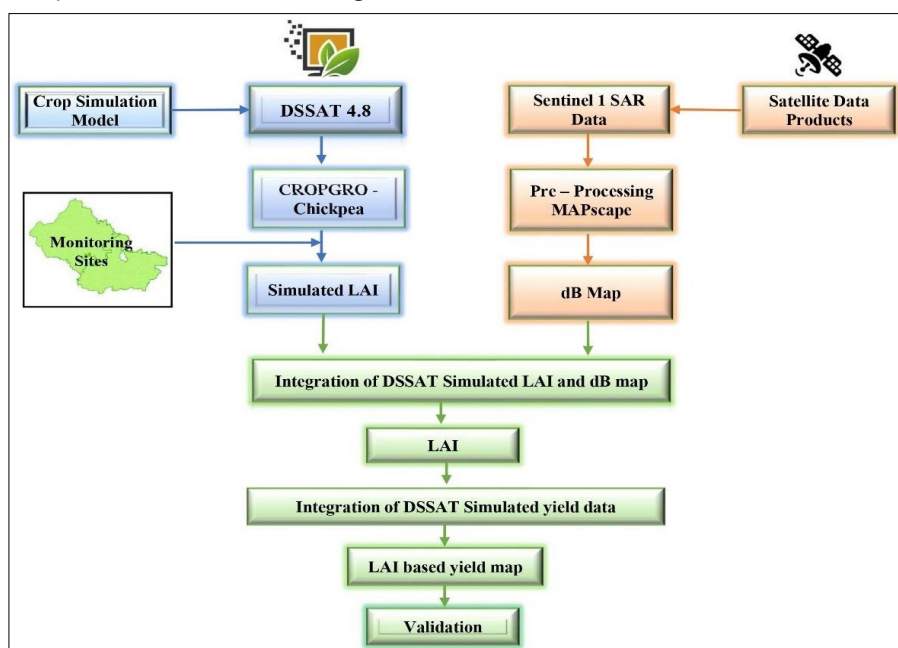


**Fig. 9.** Schematic representation of the chickpea yield estimation by integrating SAR satellite products and the DSSAT CROPGRO-Chickpea model.

## Results and Discussion

### Mapping chickpea area using SAR data

High-resolution Sentinel-1A SAR satellite data with VH polarization were used to generate accurate crop area maps for the Vidisha district during the *Rabi* season of 2022–23. Temporal backscattering values revealed distinct patterns across chickpea growth stages. The backscattering coefficient increased from the branching to flowering stage, rose slightly during pod formation and declined at maturity due to surface roughness caused by pod exposure. The temporal backscatter trends for the *Rabi* season are presented in Table 2 and Fig. 10. Temporal backscattering values extracted for monitoring sites in VH polarization showed a mean backscattering value of -18.66 dB during the seedling stage, which increased to -17.76 dB at peak flowering and dropped to -19.79 dB at maturity. The maximum and minimum dB values across all stages were -13.18 and -21.63 respectively (Table 3 and Fig. 11).

### Multi-temporal feature extraction

Multitemporal features, including minimum (VH min), maximum (VH max), span ratio and mean (VH mean), were extracted from VH polarization images. The VH max values ranged from -17.61 to -15.07 dB and VH min values ranged from -19.68 to -16.69 dB. The VH span ratio ranged from 2.08 - 5.64. The extracted features are detailed in Table 4. The 5 temporal feature values from monitoring locations were used

to determine parameter selection, enabling the classification of rice pixels and the creation of rice area maps (19). Studies used X and C-band SAR data to efficiently extract MTF (in dB) from rice monitoring fields, which they used for rice categorization (14, 20). Using C-band SAR data, research extracted MTF features from maize (21, 22).

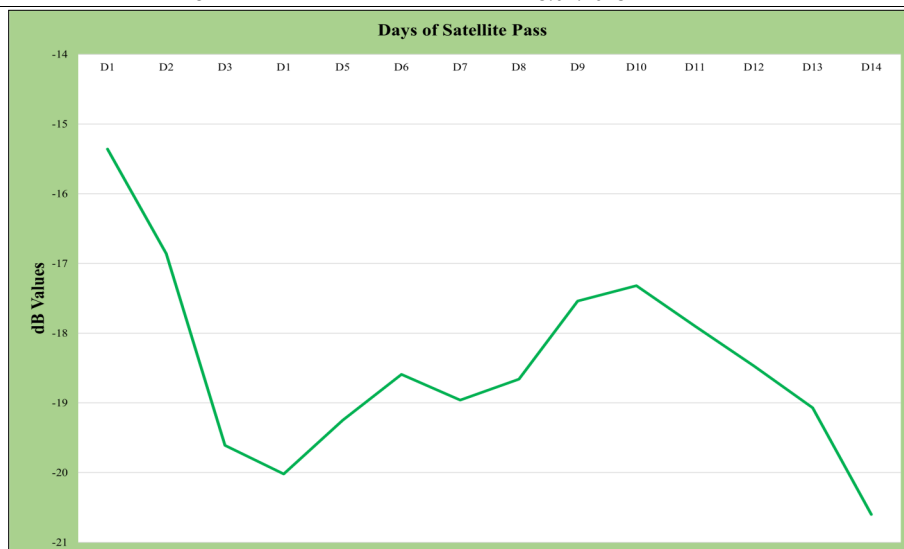
### Area estimation of chickpea

A thematic map was developed using classified SAR data to facilitate easy interpretation by end user. Additional characteristics related to different classes were derived from classified map. This study used the maximum likelihood classifier (MLC) to extract information from multi-temporal Sentinel-1A SAR data. The obtained results were analyzed and reported below. A chickpea area map for the study region was generated using multi-temporal Sentinel-1A SAR imagery. Area statistics were done for the blocks of Vidisha district. Blockwise chickpea area maps and statistics were extracted for the Basoda, Vidisha, Sironj, Lateri and Korwai blocks of Vidisha using administrative boundaries shapefiles.

The total classified chickpea area in Vidisha district was estimated at 109112 ha. Basoda had the largest chickpea area among the 5 blocks at 35386 ha, followed by Vidisha block with 24040 ha. Sironj and Lateri blocks recorded 19602 and 15357 ha of chickpea area respectively. Korwai block accounted for 14727 ha of chickpea area (Table 5 & Fig. 12).

**Table 2.** Chickpea crop temporal dB value during *Rabi* season 2022 in Vidisha district

S. No.	Satellite pass	Acquisition date	dB values
1.	D1	29.08.2022	-14.94
2.	D2	10.09.2022	-15.13
3.	D3	22.09.2022	-16.00
4.	D4	04.10.2022	-17.56
5.	D5	16.10.2022	-18.23
6.	D6	28.10.2022	-18.66
7.	D7	09.11.2022	-18.41
8.	D8	21.11.2023	-18.35
9.	D9	03.12.2023	-18.03
10.	D10	15.12.2023	-17.76
11.	D11	27.12.2023	-18.09
12.	D12	08.01.2023	-18.54
13.	D13	01.02.2023	-18.58
14.	D14	13.02.2023	-18.66
15.	D15	25.02.2023	-19.79

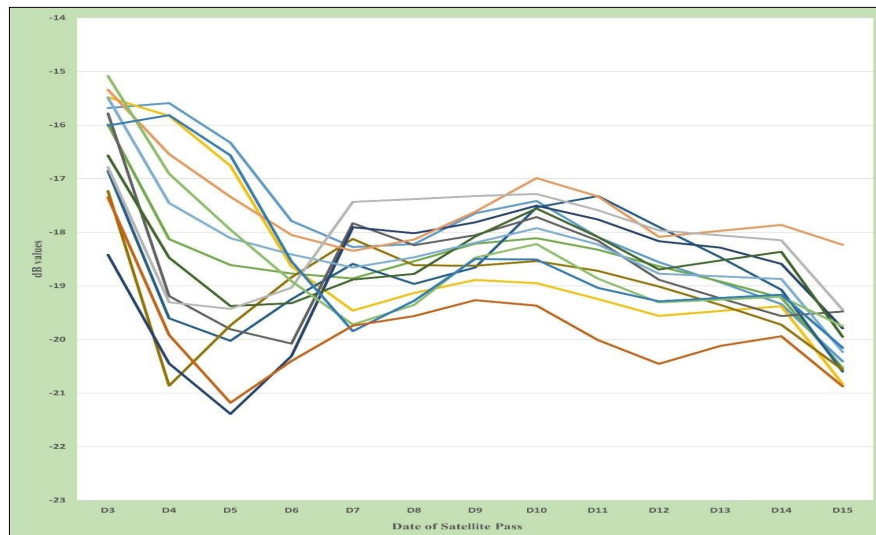


**Fig. 10.** Chickpea crop Multi-temporal dB signature during *Rabi* season in 2022.



**Table 3.** Temporal dB values of monitoring chickpea fields in Vidisha district during *Rabi* season, 2022

Fields	D1	D2	D3	D4	D5	D6	D7	D8	D9	D10	D11	D12	D13	D14	D15	Max	Min	Max-Min
1	-15.82	-15.75	-15.68	-15.59	-16.33	-17.79	-18.28	-18.22	-17.65	-17.42	-18.09	-18.56	-18.93	-19.34	-20.41	-15.59	-20.41	4.82
2	-14.75	-14.66	-14.76	-15.11	-16.34	-17.89	-17.99	-17.81	-17.48	-17.45	-17.60	-17.63	-17.70	-17.85	-19.24	-14.66	-19.24	4.59
3	-14.07	-15.24	-16.14	-16.76	-17.19	-17.51	-17.40	-17.13	-16.38	-16.03	-16.72	-17.40	-16.81	-16.30	-16.99	-14.07	-17.51	3.44
4	-15.88	-15.51	-15.48	-15.83	-16.76	-18.64	-19.46	-19.13	-18.89	-18.95	-19.24	-19.56	-19.47	-19.38	-20.83	-15.48	-20.83	5.35
5	-15.04	-14.68	-14.67	-15.03	-15.60	-16.37	-16.47	-16.41	-16.35	-16.05	-16.15	-16.57	-16.36	-16.15	-17.89	-14.67	-17.89	3.22
6	-14.05	-14.38	-15.99	-18.13	-18.61	-18.77	-18.86	-18.54	-18.21	-18.11	-18.33	-18.63	-18.92	-19.22	-20.53	-14.05	-20.53	6.48
7	-15.38	-15.36	-16.86	-19.61	-20.02	-19.25	-18.59	-18.96	-18.66	-17.54	-17.32	-17.90	-18.47	-19.07	-20.60	-15.36	-20.60	5.24
8	-14.57	-14.57	-15.91	-18.46	-19.15	-19.28	-19.42	-19.30	-19.08	-19.27	-19.85	-20.12	-20.22	-20.32	-21.63	-14.57	-21.63	7.06
9	-14.22	-14.11	-15.78	-19.19	-19.81	-20.08	-17.83	-18.24	-18.05	-17.72	-18.16	-18.88	-19.23	-19.56	-19.48	-14.11	-20.08	5.97
10	-15.09	-15.27	-17.23	-20.86	-19.73	-18.84	-18.12	-18.61	-18.63	-18.54	-18.72	-19.01	-19.35	-19.72	-20.57	-15.09	-20.86	5.77
11	-17.92	-17.68	-18.42	-20.45	-21.39	-20.31	-17.90	-18.02	-17.81	-17.51	-17.76	-18.17	-18.29	-18.59	-19.79	-17.51	-21.39	3.88
12	-15.38	-15.66	-16.57	-18.47	-19.38	-19.32	-18.88	-18.78	-18.08	-17.56	-18.09	-18.69	-18.53	-18.36	-19.95	-15.38	-19.95	4.57
13	-14.22	-14.31	-15.49	-17.45	-18.11	-18.41	-18.66	-18.46	-18.20	-17.92	-18.23	-18.77	-18.82	-18.87	-20.23	-14.22	-20.23	6.01
14	-14.30	-14.64	-15.34	-16.54	-17.34	-18.05	-18.35	-18.14	-17.62	-16.99	-17.33	-18.09	-17.97	-17.86	-18.24	-14.30	-18.35	4.04
15	-13.18	-14.76	-16.79	-19.30	-19.43	-19.03	-17.43	-17.38	-17.33	-17.28	-17.59	-17.97	-18.06	-18.15	-19.45	-13.18	-19.45	6.27
16	-14.25	-14.06	-14.53	-15.31	-15.80	-16.66	-17.00	-16.98	-16.96	-16.81	-17.12	-17.61	-17.40	-17.33	-18.97	-14.06	-18.97	4.92
17	-16.24	-15.97	-15.92	-16.45	-17.82	-19.17	-18.30	-18.66	-19.05	-18.00	-17.67	-18.27	-18.53	-18.80	-20.29	-15.92	-20.29	4.37
18	-13.68	-14.17	-15.09	-16.91	-17.95	-18.91	-19.72	-19.36	-18.47	-18.22	-18.86	-19.31	-19.25	-19.20	-19.75	-13.68	-19.75	6.07
19	-16.72	-16.43	-16.01	-15.81	-16.57	-18.54	-19.84	-19.28	-18.50	-18.51	-19.04	-19.29	-19.23	-19.16	-20.16	-15.81	-20.16	4.34
20	-13.96	-15.35	-17.35	-19.91	-21.18	-20.40	-19.74	-19.56	-19.27	-19.37	-20.01	-20.45	-20.12	-19.94	-20.87	-13.96	-21.18	7.22

**Fig. 11.** Chickpea dB curves at monitoring fields during *Rabi* season in 2022.

### Assessment of accuracy

The accuracy assessment for the chickpea area map was steered with the chickpea and non-chickpea class-based ground truth points. Using the random stratified sampling method, 150 chickpea and 100 non-chickpea points were observed and considered for validation in the study area. The overall map accuracy for the chickpea area was 86.8 %, with an average reliability of 86.10 %. A measure of excellence of classification, such as the kappa index, was identified (0.74), indicating the estimation with reasonable accuracy in the Vidisha district during *Rabi* season 2022 (Table 6). This might be due to Sentinel-1A GRD data with a 20 m resolution and its multitemporal characteristics. The overall accuracy for wheat, chickpea and mustard estimation area was 84 % when the Spectral Matching Technique (SMT) was used (23).

### LAI of chickpea at spatial level retrieved from SAR data

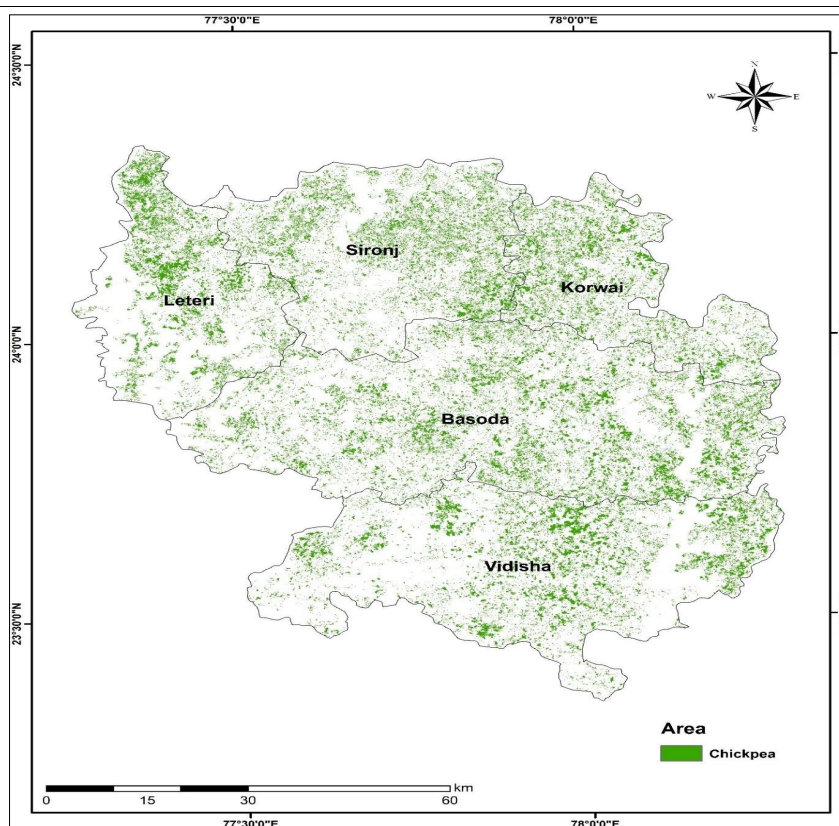
Leaf area index (LAI) and production ( $\text{kg ha}^{-1}$ ) for the 20 monitoring locations of the study area were simulated using the DSSAT CROPGRO-Chickpea model for the *Rabi* season of 2022. According to the approach, the dynamic fluctuation of chickpea growth throughout the study region was successfully captured by Sentinel-1A backscattering (dB) measurements. The backscattering values at the monitoring locations were compared to the corresponding simulated values for validation. LAI values were spatially estimated across the research area by integrating the backscattering values with DSSAT-simulated monitoring locations. The maximum backscatter and the simulated LAI were determined for each monitoring site. A linear regression equation was subsequently developed to estimate spatial LAI

**Table 4.** Minimum, maximum and mean values of multi-temporal features

Multi-Temporal Features	Minimum	Maximum	Mean
VH max	-17.617	-15.079	-17.61
VH mean	-17.928	-15.401	-16.62
VH max date	3 <sup>rd</sup> December,2022	1 <sup>st</sup> February,2023	-
VH min date	22 <sup>nd</sup> September,2022	9 <sup>th</sup> November,2022	-
VH span ratio	2.087	5.64	3.91
VH min	-19.683	-16.691	-18.08

**Table 5.** Block-wise chickpea area for Vidisha district during *Rabi* season 2022

S.No	Block name	Area (ha)	Distribution percentage over chickpea area (per cent)
1	Basoda	35386	32.43
2	Vidisha	24040	22.03
3	Sironj	19602	17.97
4	Lateri	15357	14.07
5	Korwai	14727	13.50
	Total Area	109112	100.00

**Fig. 12.** Chickpea area map of Vidisha district during *Rabi* season 2022.**Table 6.** Accuracy assessment confusion matrix of chickpea classification using SAR satellite imagery

Actual class from survey	Predicted class from the map		Accuracy (%)
	Chickpea	Non-Chickpea	
Chickpea	129	21	86
Non-chickpea	12	88	88
Reliability	91.50 %	80.70 %	86.8
Average accuracy	87.00 %		
Average reliability	86.10 %		
Overall accuracy	86.80 %		Good accuracy
Kappa index	0.74		Good accuracy

from Sentinel-1A SAR data (Fig. 13). This regression model was then employed to predict yield using the DSSAT-simulated yield and the LAI derived from SAR data (Fig. 14).

The LAI values derived from remote sensing products ranged from 2.4 - 5.3, with a mean value of 3.7 across the study area (Table 7 and Fig. 15). Remote sensing-based validation of LAI was performed by correlating the estimated values with observed LAI measurements. The overall agreement between the two was 89.1 %, while the  $R^2$ , RMSE and Normalized Root Mean Squared Error (NRMSE) were 0.51, 0.51 and 13.7 %, respectively. Previous studies' empirical relationship between LAI and backscattering coefficients indicates that ASAR data can be used for large-scale crop LAI monitoring (24). C-band SAR data can be a potential substitute for optical remote sensing data (25). Additionally, LAI retrieval using multi-polarized C-band SAR data has been demonstrated in earlier research, aligning with the results of the current investigation (26).

### Spatial level chickpea yield estimation

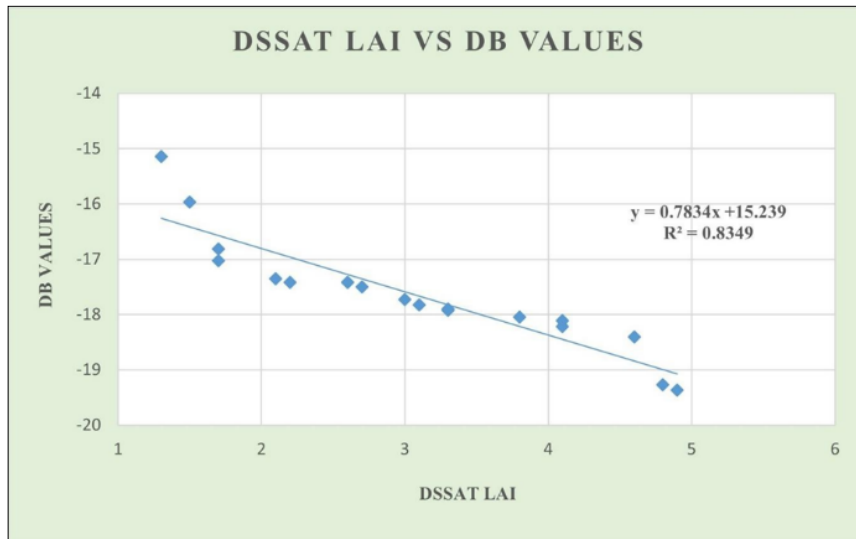
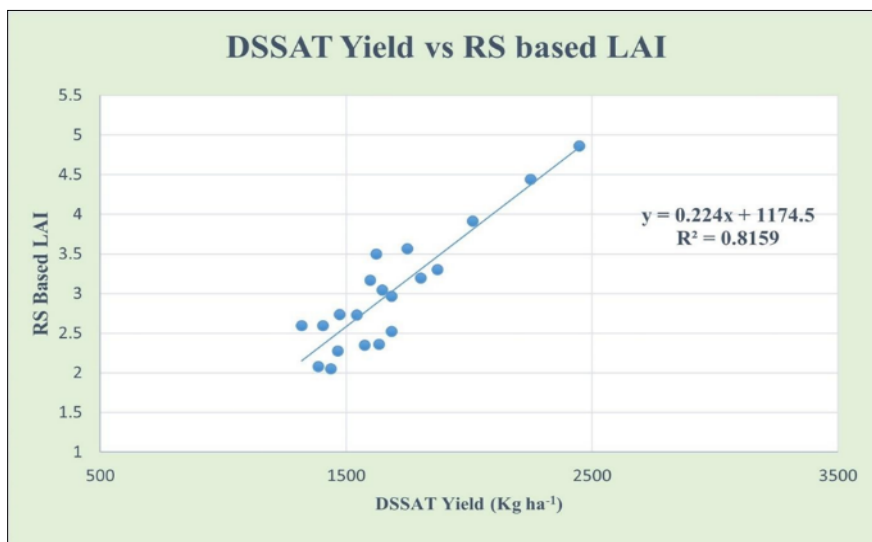
Spatial chickpea crop yield estimates were generated using a regression model integrating spatial LAI derived from remote sensing with DSSAT-based yield simulations from the CROPGRO-Chickpea model. The regression model was applied across the study area using spatially developed LAI to produce spatial chickpea yield estimates (Fig. 16). Integrating remote sensing tools with the DSSAT-CROPGRO model enabled end-of-season chickpea yield predictions. Simulated chickpea yields ranged from 1410 - 2449 kg ha<sup>-1</sup>, while yield estimates specifically for the Vidisha region varied between 1420 kg ha<sup>-1</sup> and 2330 kg h<sup>-1</sup>, with a mean yield of 1784 kg ha<sup>-1</sup>. The agreement between observed yields at monitoring locations and satellite-derived spatial yields ranged from 85.7 % - 98.3 %, with a mean agreement of 91.7 %. The model evaluation metrics, including  $R^2$ , RMSE and NRMSE, yielded average values of 0.8, 170.8 kg ha<sup>-1</sup> and 9.8 %, respectively (Table 8).

**Table 7.** Validation of remote sensing-based LAI during *Rabi* 2022

S. No	Latitude	Longitude	RS LAI	Observed LAI	Agreement (%)
1	23.7486	78.1113	3.1	3.2	96.9
2	23.6861	77.9160	3.4	3.8	89.5
3	23.6528	77.9792	2.8	2.7	96.4
4	23.8198	77.8703	2.4	2.7	88.9
5	23.6683	77.7984	3.0	2.4	80.0
6	23.8221	77.7537	5.3	4.2	79.2
7	24.0682	77.7557	2.8	3.2	87.5
8	24.0375	77.5337	5.0	4.8	96.0
9	23.6335	78.0807	3.5	3.1	88.6
10	24.1179	77.6852	3.4	3.6	94.4
11	24.0096	78.0008	4.2	4.8	87.5
12	23.7796	77.9331	4.5	3.7	82.2
13	23.8131	78.0272	3.7	4.2	88.1
14	23.9754	77.5929	3.5	4.0	87.5
15	24.0905	77.9180	4.3	4.7	91.5
16	23.9652	77.9130	3.9	4.2	92.9
17	23.5890	77.9564	4.3	4.0	93.0
18	23.9555	78.0470	3.4	4.4	77.3
19	23.8368	77.9640	4.6	4.3	93.5
20	23.8933	78.0273	3.5	3.8	92.1
<b>Mean</b>			4	3.8	89.1
<b>R<sup>2</sup></b>				0.5	
<b>RMSE</b>				0.5	
<b>NRMSE (%)</b>				13.7	

**Table 8.** Validation of remote sensing-based yield during *Rabi* 2022

S. No	Latitude	Longitude	Observed yield (kg ha <sup>-1</sup> )	RS yield (kg ha <sup>-1</sup> )	Agreement (%)
1	23.7486	78.1113	1320	1420	93.0
2	23.6861	77.9160	1720	1620	94.2
3	23.6528	77.9792	1480	1710	86.5
4	23.8198	77.8703	1467	1650	88.9
5	23.6683	77.7984	1290	1450	89.0
6	23.8221	77.7537	2720	2330	85.7
7	24.0682	77.7557	1510	1720	87.8
8	24.0375	77.5337	2451	2220	90.6
9	23.6335	78.0807	1633	1750	93.3
10	24.1179	77.6852	1750	1610	92.0
11	24.0096	78.0008	1934	1830	94.6
12	23.7796	77.9331	1622	1810	89.6
13	23.8131	78.0272	1920	2070	92.8
14	23.9754	77.5929	1530	1690	90.5
15	24.0905	77.9180	1544	1680	91.9
16	23.9652	77.9130	1640	1740	94.3
17	23.5890	77.9564	1630	1530	93.9
18	23.9555	78.0470	1790	1950	91.8
19	23.8368	77.9640	2015	2110	95.5
<b>Mean</b>			1739	1784	91.7
<b>R<sup>2</sup></b>				0.8	
<b>RMSE (kg ha<sup>-1</sup>)</b>				170.8	
<b>NRMSE (%)</b>				9.8	

**Fig. 13.** Integration of DSSAT LAI with SAR maximum dB during *Rabi* 2022.**Fig. 14.** Integration of DSSAT yield with RS based LAI during *Rabi* 2022.

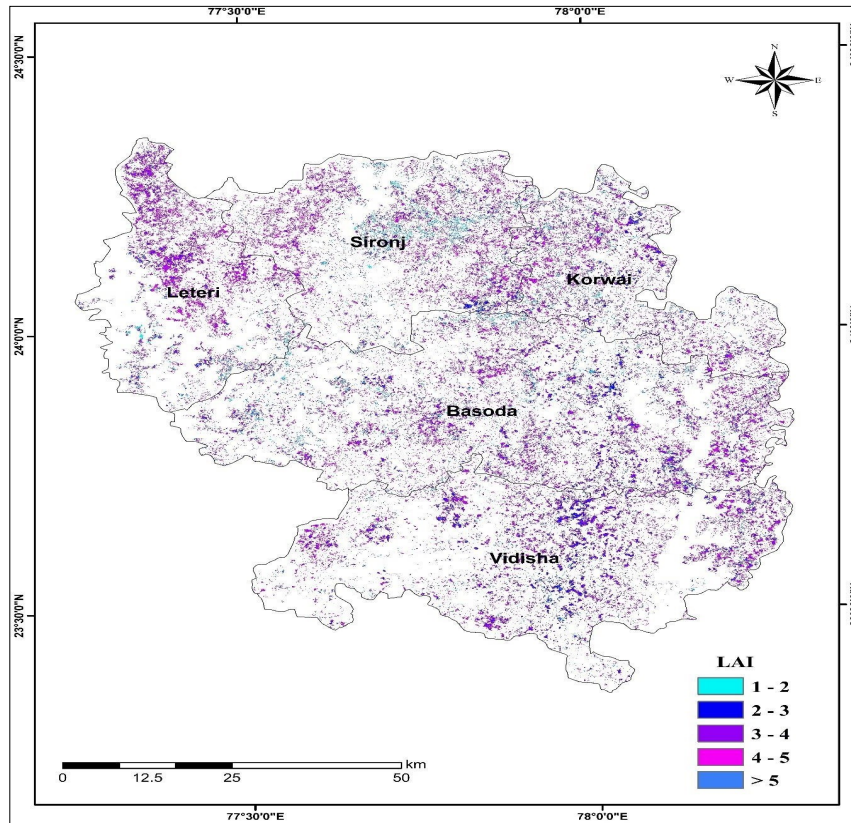


**Fig. 15.** Spatial LAI map of Vidisha district during *Rabi* 2022.

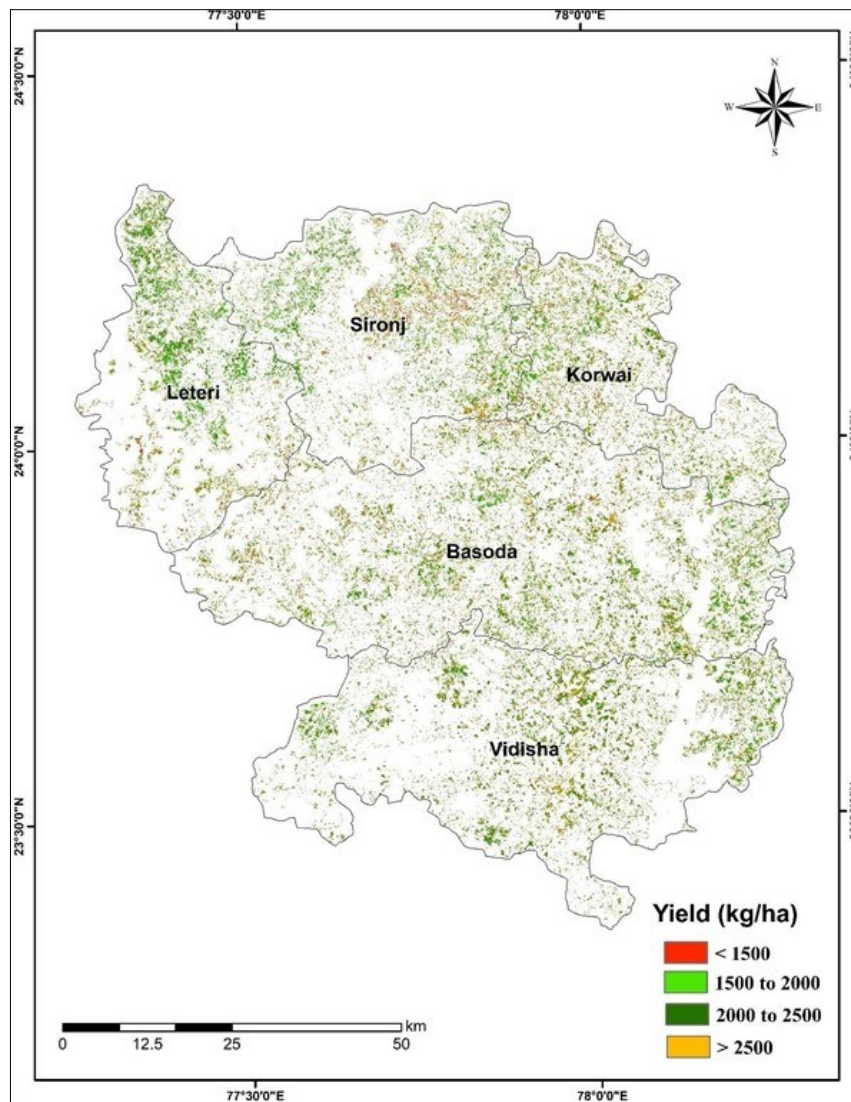


**Fig. 16.** Spatial yield map of Vidisha district during *Rabi* 2022.

Previous studies have demonstrated the effectiveness of integrating remote sensing-derived LAI with crop simulation models. For example, according to a study, utilized remote sensing-derived LAI with the CERES model to estimate winter wheat yield (27). In contrast, according to another study, successfully incorporated SAR-derived LAI to evaluate groundnut yield by integrating it with the DSSAT model (28). Despite variations in monitoring locations and growing conditions, Sentinel-1A SAR data proved reliable for estimating chickpea areas in the Vidisha district. When integrated with the DSSAT-CROPGRO-Chickpea crop simulation model, this approach provided reasonably accurate spatial yield estimates for chickpeas in the region, highlighting its potential for broader agricultural applications.

## Conclusion

Integrating Sentinel-1A SAR remote sensing products with the DSSAT CROPGRO-Chickpea crop simulation model provides a robust framework for accurate crop area and yield estimation. This approach overcomes the limitations of traditional survey methods by delivering high-resolution, weather-independent data for efficient and precise agricultural monitoring. Temporal backscatter trends captured from radar data effectively characterized chickpea growth stages, from emergence to maturity, demonstrating significant dynamic variations. The study successfully mapped a total chickpea cultivation area of 109112 ha, achieving an overall classification accuracy of 86.8 % with a Kappa index 0.74.

Integrating remote sensing-derived LAI with the DSSAT model enabled precise spatial yield estimations, with simulated yields ranging from 1410 - 2449 kg ha<sup>-1</sup>. Strong agreements were observed between simulated and ground-measured values, with an average agreement of 91.7 % for yield and 89.1 % for LAI. This validation confirms the reliability of combining SAR data and crop models for operational crop monitoring and yield forecasting.

This methodology enhances agricultural planning and resource allocation while supporting early warning systems and promoting sustainable farming practices. The results of this study provide a foundation for expanding integrated approaches to other crops and regions, contributing to enhanced food security and resilience to climate variability.

## Acknowledgements

We thank the "MNCFC - Pilot Studies for GP level crop estimation using advanced technologies for non-cereal crops" project for funding this research.

## Authors' contributions

SP carried out the experiment observation and drafted the manuscript and guided the research by formulating the concept and approved the final manuscript. AR conceived the study and participated in its design and coordination.

NSS performed the statistical analysis. SS conceived the study and participated in its design and coordination. KM participated in the data analysis and revised manuscript. KPR guided the research by formulating the research concept and helped secure funds. All authors reviewed the results and approved the final version of the manuscript.

## Compliance with ethical standards

**Conflict of interest:** The authors declare no conflict of interest.

**Ethical issues:** None

## References

- Jukanti AK, Gaur PM, Gowda C, Chibbar RN. Nutritional quality and health benefits of chickpea (*Cicer arietinum* L.): A review. *Br J Nutr.* 2012;108(S1):S11–26. <https://doi.org/10.1017/S0007114512000797>
- Lark TJ, Schelly IH, Gibbs HK. Accuracy, bias and improvements in mapping crops and cropland across the United States using the USDA Cropland Data Layer. *Remote Sens.* 2021;13(5):968. <https://doi.org/10.3390/rs13050968>
- Gaur PM, Tripathi S, Gowda CL, Rao GR, Sharma H, Pande S, et al. Chickpea seed production manual. Tropical Legumes II Project. 2010. p. 28. Available from: <https://oar.icrisat.org/id/eprint/10276>
- Merga B, Haji JJ. Economic importance of chickpea: production, value and world trade. *Cogent Food Agric.* 2019;5(1):1615718. <https://doi.org/10.1080/23311932.2019.1615718>
- Directorate of Economics and Statistics, Ministry of Agriculture and Farmers Welfare, Government of India [Internet]. New Delhi: GOI; 2021 [cited 2025 Feb 24].
- Karthikeyan L, Chawla I, Mishra AK. A review of remote sensing applications in agriculture for food security: crop growth and yield, irrigation and crop losses. *J Hydrol.* 2020;586:124905. <https://doi.org/10.1016/j.jhydrol.2020.124905>
- Peng D, Huang J, Li C, Liu L, Huang W, Wang F, et al. Modelling paddy rice yield using MODIS data. *Agric For Meteorol.* 2014;184:107–16. <https://doi.org/10.1016/j.agrformet.2013.09.006>
- Setiyono TD, Quicho ED, Gatti L, Campos-Taberner M, Busetto L, Collivignarelli F, et al. Spatial rice yield estimation based on MODIS and Sentinel-1 SAR data and ORYZA crop growth model. *Remote Sens.* 2018;10(2):293. <https://doi.org/10.3390/rs10020293>
- Pazhanivelan S, Geethalakshmi V, Tamilmounika R, Sudarmanian N, Kaliaperumal R, Ramalingam K, et al. Spatial rice yield estimation using multiple linear regression analysis, semi-physical approach and assimilating SAR satellite-derived products with DSSAT crop simulation model. *Agron.* 2022;12(9):2008. <https://doi.org/10.3390/agronomy12092008>
- Raviz J, Mabalay MR, Laborte A, Nelson A, Holecz F, Quilang EJ, et al. Mapping rice areas in Mindanao using the first images from Sentinel-1A: The PRISM Project experience. In: 36th Asian Conference on Remote Sensing (ACRS); 2015 Oct 19; Manila. p. 19-23.
- Holecz F, Barbieri M, Collivignarelli F, Gatti L, Nelson A, Setiyono TD, et al. An operational remote sensing based service for rice production estimation at national scale. In: Proceedings of the living planet symposium; 2013 Sep.
- De Grandi G, Leysen M, Lee J, Schuler D. Radar reflectivity estimation using multiple SAR scenes of the same target: technique and applications. *IGARSS'97 IEEE Int Geosci Remote Sens Symp Proc Remote Sens.* 1997;2:1047–50. <https://doi.org/10.1109/IGARSS.1997.615338>
- Aspert F, Bach-Cuadra M, Cantone A, Holecz F, Thiran J-P. Time-

- varying segmentation for mapping of land cover changes. ENVISAT Symposium; 2007. <https://infoscience.epfl.ch/handle/20.500.14299/7580>
14. Nelson A, Setiyono T, Rala AB, Quicho ED, Raviz JV, Abonete PJ, et al. Towards an operational SAR-based rice monitoring system in Asia: examples from 13 demonstration sites across Asia in the RIICE project. *Remote Sens.* 2014;6(11):10773–812. <https://doi.org/10.3390/rs61110773>
  15. Congalton RG. A review of assessing the accuracy of classifications of remotely sensed data. *Remote Sens Environ.* 1991;37(1):35–46. [https://doi.org/10.1016/0034-4257\(91\)90048-B](https://doi.org/10.1016/0034-4257(91)90048-B)
  16. Lillesand T, Kiefer RW, Chipman J. *Remote sensing and image interpretation.* 7th Edition, New York: Wiley; 2015.
  17. Jones JW, Hoogenboom G, Porter CH, Boote KJ, Batchelor WD, Hunt L, et al. The DSSAT cropping system model. *Eur J Agron.* 2003;18(3-4):235–65. [https://doi.org/10.1016/S1161-0301\(02\)00107-7](https://doi.org/10.1016/S1161-0301(02)00107-7)
  18. De Kauwe M, Disney M, Quaife T, Lewis P, Williams M. An assessment of the MODIS collection 5 leaf area index product for a region of mixed coniferous forest. *Remote Sens Environ.* 2011;115(2):767–80. <https://doi.org/10.1016/j.rse.2010.11.004>
  19. Pazhanivelan S, Kannan P, Mary PCN, Subramanian E, Jeyaraman S, Nelson A, et al. Rice crop monitoring and yield estimation through COSMO Skymed and TerraSAR-X: A SAR-based experience in India. *Int Arch Photogramm Remote Sens Spatial Inf Sci.* 2015;40:85–92. <https://doi.org/10.5194/isprsarchives-XL-7-W3-85-2015>
  20. Tamilmounika R, Pazhanivelan S, Rangunath K, Sivamurugan A, Sudarmanian N, Kumaraperumal R, et al. Paddy area estimation in Cauvery Delta region using synthetic aperture radar. *Eco Env Cons.* 2022;28:517–22. <http://doi.org/10.53550/EEC.2022.v28i01s.069>
  21. Venkatesan M, Pazhanivelan S, Sudarmanian N. Multi-temporal feature extraction for precise maize area mapping using time-series Sentinel-1A SAR data. *Int Arch Photogramm Remote Sens Spatial Inf Sci.* 2019;42:169–73. <https://doi.org/10.5194/isprs-archives-XLII-3-W6-169-2019>
  22. Thirumeninathan S, Pazhanivelan S, Sudarmanian N, Rangunath K, Gurusamy A, Sritharan N. Rabi groundnut area estimation using synthetic aperture radar (SAR) in Thiruvannamalai district of Tamil Nadu. *Legume Res Int J.* 2022;45(3):319–26. <https://doi.org/10.18805/LR-4746>
  23. Gumma MK, Kadiyala M, Panjala P, Ray SS, Akuraju VR, Dubey S, et al. Assimilation of remote sensing data into crop growth model for yield estimation: A case study from India. *J Indian Soc Remote Sens.* 2021;50(2):257–70. <https://doi.org/10.1007/s12524-021-01341-6>
  24. Lin H, Chen J, Pei Z, Zhang S, Hu X. Monitoring sugarcane growth using ENVISAT ASAR data. *IEEE Trans Geosci Remote Sens.* 2009;47(8):2572–80. <https://doi.org/10.1109/TGRS.2009.2015769>
  25. Chen J, Lin H, Huang C, Fang C. The relationship between the leaf area index (LAI) of rice and the C-band SAR vertical/horizontal (W/HH) polarization ratio. *Int J Remote Sens.* 2009;30(8):2149–54. <https://doi.org/10.1080/01431160802609700>
  26. Leonard A, Waldner F, Jacques DC, Defourny P. Crop identification and growth monitoring along the season with RADARSAT-2 Quad-Polarised time series in Belgium. *IGARSS.* 2014. <http://hdl.handle.net/2078.1/147321>
  27. Yang H, Dobermann A, Cassman KG, Walters DT. Features, applications and limitations of the hybrid-maize simulation model. *Agron J.* 2006;98(3):737–48. <https://doi.org/10.2134/agronj2005.0162>
  28. Thirumeninathan S, Pazhanivelan S, Mohan R, Pouchepparadjou A, Sudarmanian NS, Rangunath K, et al. Integrating S1A microwave remote sensing and DSSAT CROPGRO simulation model for groundnut area and yield estimation. *Eur J Agron.* 2024;161:127348. <https://doi.org/10.1016/j.eja.2024.127348>

#### Additional information

**Peer review:** Publisher thanks Sectional Editor and the other anonymous reviewers for their contribution to the peer review of this work.

**Reprints & permissions information** is available at [https://horizonpublishing.com/journals/index.php/PST/open\\_access\\_policy](https://horizonpublishing.com/journals/index.php/PST/open_access_policy)

**Publisher's Note:** Horizon e-Publishing Group remains neutral with regard to jurisdictional claims in published maps and institutional affiliations.

**Indexing:** Plant Science Today, published by Horizon e-Publishing Group, is covered by Scopus, Web of Science, BIOSIS Previews, Clarivate Analytics, NAAS, UGC Care, etc  
See [https://horizonpublishing.com/journals/index.php/PST/indexing\\_abstracting](https://horizonpublishing.com/journals/index.php/PST/indexing_abstracting)

**Copyright:** © The Author(s). This is an open-access article distributed under the terms of the Creative Commons Attribution License, which permits unrestricted use, distribution and reproduction in any medium, provided the original author and source are credited (<https://creativecommons.org/licenses/by/4.0/>)

**Publisher information:** Plant Science Today is published by HORIZON e-Publishing Group with support from Empirion Publishers Private Limited, Thiruvananthapuram, India.